Cross-Correlation based Ultrasonic Gas Flow Sensor with Temperature Compensation

José R. García Oya, Eduardo Hidalgo Fort, Daniel Narbona Miguel, Alejandro Sainz Rojas, Ramón González Carvajal, *Fellow, IEEE*, and Fernando Muñoz Chavero, *Member, IEEE*

***Abstract*— In this paper, the design of an ultrasonic gas flow sensor with a low cost and low energy temperature compensation method based on time of flight measurement is presented. In order to minimize the cost, the proposed thermal compensation method, on the one hand, does not require a temperature sensor and, on the other hand, only requires an initial calibration at room temperature. The presented COTS (Commercial Off The Shelf) based sensor has been previously optimized at different levels: mechanical design, validation of the piezoelectric transducers and selection of the time of flight detection algorithm. As result, this paper presents a gas flow sensor based on a V-configuration pipe, using 200 kHz-piezoelectric transducers and a cross-correlation method based on the Hilbert Transform. The proposed design fully meets the accuracy requirements given by the EN14236 standard, improving the features of current commercial gas flow sensors in terms of cost, accuracy and power consumption.**

***Index Terms*—Cross-Correlation, Piezoelectric Transducers, Temperature Compensation, Transit-Time Measurement, Ultrasonic Gas Flow Sensor**

I. Introduction

Nowadays, smart meters are becoming an essential tool in terms of energy efficiency and interoperability. Ultrasonic gas flow sensors are the most suitable technology for today's interoperability needs and low cost, low power requirements [1]-[4]. The main advantage of ultrasonic sensors is that they do not require moving parts, so they need less frequent maintenance than mechanical sensors and provide higher accuracy over their lifetime. Moreover, they are non-invasive and have self-diagnosis capabilities [5].

The design of an ultrasonic gas flow sensor must address different challenges to achieve the resolution required by the EN14236 standard while minimizing cost and power consumption. Among others, it will be necessary to (1) determine the appropriate dimensions and shape, (2) select piezoelectric transducers with sufficiently low thermal drift and (3) a time of flight (ToF) detection algorithm that optimizes accuracy and power consumption. Moreover, the number of required elements should be minimized by avoiding the need of a temperature sensor if possible. Finally, to reduce manufacturing costs, a thermal compensation method is needed that only requires calibration at room temperature.

Ultrasonic gas flow sensors have been widely studied, but it is difficult to find a research work that meets all the requirements describe above. In [1], a hybrid architecture (by implementing the Z and V transducers configuration that will be described in Section III) is proposed to improve accuracy performance at the expense of increasing hardware costs. [1] improves accuracy by implementing a computationally expensive ToF detection algorithm, based on a Gauss–Newton method, which requires to be implemented in a power hungry device, such as a Field Programmable Gate Arrays (FPGA). Similarly, [2] presents a Z-configuration pipe to implement a novel least square (LS) based ToF detection algorithm optimized for low SNR scenarios. However, this method has to be implemented by an external computer, preventing its use in domestic installations. Additionally, this design employs an external temperature sensor, increasing costs and power consumption. Otherwise, works based on resource-limited embedded systems have also been published. For example, [3] achieves adequate accuracy using a low cost microcontroller, although it only provides measurements at room temperature without the ability to compensate thermal drift.

Therefore, there is a need to design an ultrasonic gas flow sensor optimized for accuracy and power consumption, and also to implement a low cost temperature compensation method. In this paper, the proposed method is directly implemented from the absolute ToF measurement, by exploiting the accuracy achieved by the previous optimization of the sensor. Other low cost temperature compensation methods have been studied in the literature. For example, [6]-[7] present a thermal compensation method based on the electrical impedance of the piezoelectric, but this technique has a higher dependence on the ultrasonic beam deviation at high flow rates, since it is based on the received amplitude. Otherwise, high-complexity techniques for temperature compensation have been recently published, such as those based on machine learning [8] or neural networks [7], which expend more computational resources and usually need an off-line compensation. This paper continues the work presented in [9], where a complete design of an ultrasonic gas flow sensor was described. In the present work, the sensor has been enhanced in terms of accuracy and the proposed thermal compensation method has been implemented over this design.

The paper is organized as follow. Section II details the

J. R. G. Oya, E. H. Fort, D. N. Miguel, A. S. Rojas, F. M. Chavero and R. G. Carvajal are with the Electronic Engineering Department, University of Seville, Sevilla, E-41092 Spain (e-mail: jose.garciaoya@gie.esi.us.es, {ehidalgo, dnarbona, asrojas, carvajal, fmunoz }@us.es).

This work was supported by the Andalusian Regional Government and the European Commission, under project PY20 RE 012 AICIA, and by Woodswallow S.L.

measurement principle and the selected detection algorithm. Section III describes the mechanical design and the transducers selection. In Section IV, experimental results are discussed. Finally, conclusions are drawn in Section V.

II. Measurement Principle

The principle of operation of ultrasonic flow sensors consists on the transmission and reception of an acoustic wave through the gas, by means of two piezoelectric transducers installed upstream (UPS) and downstream (DNS) on the pipe.

Specifically, ultrasonic transit-time flow sensors measure the difference of the propagation times of ultrasonic pulses in and against the flow direction, as shown in Figure 1. The values of the absolute ToF are given by (1), where L is the distance of the ultrasonic link, c is speed of the sound in the medium, v is the flow velocity and α is the angle of incidence. Flow Q is given by (2), where S is the pipe section. Additionally, from (3), it is possible to measure c without dependence on v. This property will be used as a basis to compensate for errors due to temperature drifts, as described in Section IV.A, from the measurement of t_{ab} and t_{ba}, i.e., c. The dependence of c on temperature T is given by (3), where γ is the adiabatic index, M is the molar mass of the gas, and R is the universal gas constant [10].

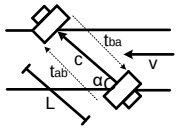

Fig. 1. Measurement principle

$$t_{ab} = \frac{L}{c + v \cdot \cos(\alpha)} \; ; \; t_{ba} = \frac{L}{c - v \cdot \cos(\alpha)} \tag{1}$$

$$Q = S \cdot v = \frac{S \cdot L}{2 \cdot \cos(\alpha)} \cdot \left(\frac{1}{t_{ab}} - \frac{1}{t_{ba}} \right) \tag{2}$$

$$c = \frac{L}{2} \cdot \left(\frac{1}{t_{ab}} + \frac{1}{t_{ba}} \right) = \sqrt{\frac{\gamma \cdot R \cdot T}{M}} \tag{3}$$

The most common solutions for implementing ultrasonic gas flow sensors are based on: 1) time-to-digital conversion (TDC), which detects zero crossings in the received signal; and 2) analog-to-digital conversion (ADC), which captures the whole received signal, stores it and post-processes it for the estimation of ToF. The ADC based approach provides, as main advantage over TDC, a higher accuracy, allowing the implementation of the correlation between both signals, which acts as a noise digital filter and presents an improved zero-flow drift performance [11]-[12].

Additionally, for this ADC based approach, Hilbert Transform (HT) is applied on the original received signal, in order to obtain its envelope of and also to improve accuracy of the ToF estimation. As is known, HT of a real signal, $\tilde{x}(t)$, can be used to obtain an analytic signal as:

$$x_a(t) = x(t) + jH[x(t)] = x(t) + j\tilde{x}(t) \tag{4}$$

And the envelope of the signal *x(t)* can be obtained from the modulus of this analytic signal. Once UPS and DNS envelopes have been obtained (corresponding to the original signals *x(t)* and *y(t)*) to estimate absolute ToFs, the HT of the signal *y(t)* also can be used for calculation of cross-correlation instead of using signal *y(t)* itself (CCF). The cross-correlation function obtained with the Hilbert Transform (CCFHT) is equal to:

$$R_{x\tilde{y}}(\tau) = CCF[x(t)\tilde{y}(t+\tau)] \tag{5}$$

As can be demonstrated, delay time τ (i.e., differential ToF (DToF) for this application) estimation by determining the maximum position of CCF can be replaced by determining the zero-crossing position of CCFHT [13], allowing a simpler and more accurate estimation, by computing a linear interpolation over few points, instead of the parabolic or Gaussian interpolations generally employed for the CCF case [14].

III. Ultrasonic Flow Sensor Design

MSP430FR6043 from Texas Instruments has been selected as the core component in the design of the flow sensor. This device offers an integrated ultrasonic sensing solution, including: a high resolution ADC for signal acquisition, a low energy digital signal processor to implement the selected cross-correlation based algorithm, a Programmable Pulse Generator (PPG), and a front-end with a Programmable Gain Amplifier (PGA). The proposed ultrasonic flow sensor based on this IC has been designed at two main levels:

A. Mechanical design

Two ultrasonic paths configurations have been tested: Z-configuration (based on a direct way between the transducers) and V-configuration (based on one reflection of the ultrasonic wave over the pipe floor). For each configuration, different geometries were analyzed, i.e., different angles of incidence, cross-sections and ultrasonic path lengths.

A V-configuration with an ultrasonic path length of 55.9 mm, a cross-section of 9.5x20.3 mm^2, and an angle of incidence of 65º was selected because it presents the best results in terms of accuracy, providing a reasonable compromise between low flow rates (where the minimum DToF has to be maximized) and high flow rates (where the effect of the ultrasonic beam deviation has to be minimized).

B. Transducer selection

Several transducers from different manufacturers at 200 kHz and 500 kHz were experimentally tested in terms of accuracy and thermal drift, and finally a 200 kHz transducer from Jiakang manufacturer was chosen. Also, working at 200 kHz offers the additional advantage of allowing a lower sampling rate (1 MHz), which contributes to lower power consumption. Another advantage is that the signal at 200 kHz is attenuated 6-9 dB less than at 500 kHz, allowing to reduce the transmitted ultrasonic signal amplitude and thus the power consumption. Zero-drift performance was also tested in order to evaluate the non-reciprocity between the transducers pairs [15]. This test consisted of measuring DToF without flow, which is theoretically 0, gradually along the temperature range (-10ºC to 40ºC), resulting in a maximum zero flow drift of 752 ps at 200 kHz and 1191 ps at 500 kHz.

Transducers have been also compared regarding the deviation between pairs measuring flow at the extreme temperatures established by the standard. Table I illustrates the

errors regarding 23ºC for different flow rates and temperatures. Note that the results obtained for the 200 kHz case are more promising in order to comply the standard specifications, which require an error <3% in the range of 40-600 l/h and <1.5% in the range of 600-7200 l/h. In other words, the maximum error obtained at 560 l/h (1.07%) provides an accuracy room of 1.93%. In the same way, the maximum error obtained at 2000 l/h (0.53%) provides an accuracy room of 0.97%. These accuracy requirements will be fully comply at 200 kHz, as described in Section IV.

TABLE I
FLOW DRIFT RESULTS COMPARISON

Frequency (kHz)	Flow (l/h)	Error at -10ºC (%)	Error at 40ºC (%)
200	560	0.64	1.07
200	2000	0.51	0.53
500	560	0.45	1.52
500	2000	0.44	0.52

IV. EXPERIMENTAL RESULTS

A. Calibration and temperature compensation

The method proposed in this section is intended to eliminate the need for calibration at different temperatures. From (2), flow could be rewritten as equations (6) and (7):

$$Q = k \cdot \Delta \quad (6)$$

$$Q = k_g \cdot \Delta \Big/ t_{ab} \cdot t_{ba} \quad (7)$$

where Δ is DToF, $k_g = S \cdot L/2 \cdot \cos(\alpha)$ and $k = k_g/t_{ab} \cdot t_{ba} \approx k_g/c^2$. Thus, measuring flow from (6), with k obtained for flow adjustment at 23ºC, the errors caused by temperature variations will be very pronounced, because, from (3), c strongly depends on temperature. In this paper, the proposed method is based on using (7) by the measurement of t_{ab}, t_{ba} and Δ. Theoretically, using (7), the dependence on temperature would be eliminated and it would only be necessary to calibrate at room temperature. Although the error due to temperature variations (with a maximum of 4.2% for all the tested flow rates and temperatures) is greatly decreased by using (7), comparing with the case of using (6) (with a maximum error of 12.1%), the obtained error is still higher than the admitted by the standard, so it is necessary an additional temperature statistical compensation.

In order to reduce costs, the proposed method is based on calibrating only at room temperature and using the value of $t_{ab}+t_{ba}$, which is approximately $2 \cdot L/c$, as an indirect temperature measurement in order to avoid the use of an external temperature sensor. The proposed method is based on the following steps:

1) Preliminarily, by using a climatic chamber, several sensors have been tested for N nominal temperatures and M nominal flow rates specified by the standard, calculating each k_g to eliminate the error regarding the flow reference. Then, the average of the maximum and the minimum of the percentages variations to correct k_g for each pair (Δ, $t_{ab}+t_{ba}$) is calculated in order to minimize the maximum error. At the end of this measurement campaign, an unique MxN matrix α (where nominal Δ corresponds with the rows and nominal $t_{ab}+t_{ba}$ with the columns) will be available, with each element α_{ij} corresponding with the correction factor to apply over each k_g adjusted at 23ºC of a specific sensor.

2) For a specific sensor, its calibration at 23ºC is performed by using (7), in order to extract a matrix $k_{g1xM}=[k_{g1}..k_{gi}...k_{gM}]$ at the nominal flows given by the standard. Then, matrix α is applied, so the resulting nominal k_g are given by $k_g\_ref_{ij}=k_{gi} \cdot \alpha_{ij}$.

3) Finally, in order to compensate at any intermediate flow and temperature, the proposed method is implemented by using an interpolation by planes, where axis x is Δ, axis y is $t_{ab}+t_{ba}$ and axis z is $k_g\_ref_{ij}$. A 4-equations system is solved to calculate the coefficients (a, b, c, d):

$$\begin{aligned} &a \cdot \Delta_i + b \cdot (t_{ab}+t_{ba})_j + c \cdot \Delta_i \cdot (t_{ab}+t_{ba})_j + d = k_g\_ref_{i,j} \\ &a \cdot \Delta_{i+1} + b \cdot (t_{ab}+t_{ba})_j + c \cdot \Delta_{i+1} \cdot (t_{ab}+t_{ba})_j + d = k_g\_ref_{i+1,j} \\ &a \cdot \Delta_i + b \cdot (t_{ab}+t_{ba})_{j+1} + c \cdot \Delta_i \cdot (t_{ab}+t_{ba})_{j+1} + d = k_g\_ref_{i,j+1} \\ &a \cdot \Delta_{i+1} + b \cdot (t_{ab}+t_{ba})_{j+1} + c \cdot \Delta_{i+1} \cdot (t_{ab}+t_{ba})_{j+1} + d = k_g\_ref_{i+1,j+1} \end{aligned} \quad (8)$$

where Δ and $t_{ab}+t_{ba}$ are the nominal values. After solving these MxN 4-equations systems (for the MxN possible segments), $4xMxN$ coefficients are stored in the memory of the sensor. Then, for any intermediate measured values of Δ and $t_{ab}+t_{ba}$ its corresponding segment is determined (i.e., the coefficients to be used), to calculate the interpolated value of $k_g\_ref_{ij}$, which is finally applied in (7) to flow calculation. Table II shows the achieved accuracy in the case of only using (7) (with kg calibrated at 23ºC) and in the case of using the proposed compensation method, based on $k_g\_ref_{ij}$. Note that the errors showed in Table II for each flow rate correspond with the maximum for the different tested designs and temperatures. Finally, Figure 2 illustrates the achieved errors by using $k_g\_ref_{ij}$ for different temperatures and flow rates.

TABLE II
TEMPERATURE COMPENSATION RESULTS

Flow rate (l/h)	40	80	200	560	1440	2880	4000	6000	7200
Using (7)	3.6	3.9	3.8	3.5	2.3	3.9	4	4.1	4.2
Using kg_ref_{ij}	0.9	0.8	0.3	0.7	0.5	0.5	0.6	0.6	0.4

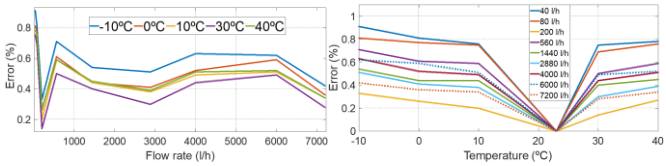

Fig. 2. Achieved errors for different temperatures (left) and flow rates (right)

B. Accuracy results and discussion

By the integration of the all previously designed parts, the final design was tested, achieving the accuracy results illustrated in Figure 3, where it is possible to observe how the standard EN14236 specifications are fulfilled. Specifically, the proposed sensor presents a maximum error of 1.8% at 40 l/h (leading to a resolution of 0.72 l/h and 415.6 ns), <1% in the range 80-600 l/h and <0.5% in the range 600-7200 l/h. In Figure 3, dash line sets the error admitted by the standard (averaging 6 measurements), and dots are the achieved errors by using the average of 6 samples, for the cases of one and four measurements of DToF per flow measurement. Moreover, note that adding the error due to temperature drift

(0.9% at 40 l/h from Table II) the standard requirements is still completely fulfilled. Additionally, the non-linear error has been measured, resulting in a maximum of 2.24 l/h at 1440 l/h.

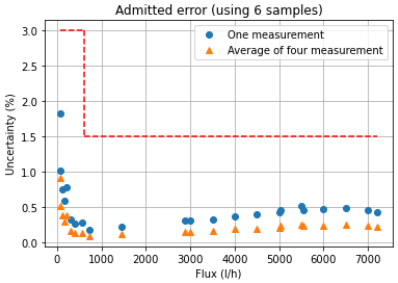

Fig. 3. Achieved accuracy

This value of 4 measurements each 2 seconds was selected after experimentally measuring the power consumption, resulting in 21.4 µA per flow measurement for the implemented HT based method (with a data processing time of 16.1 ms), lower than other commercial ultrasonic flow sensors, such as Panasonic F9CM62A and Maxim MAX35104, which report, respectively, 25.7 µA and 31 µA. Thus, although performing one measurement each 2 seconds the requirements are fulfilled, it would possible to perform up to 4 measurements in order to consume around the 30% of the total power budget, considering a standard battery of 17A·h for 15 years, i.e., consuming 4.8 A·h for its lifetime.

Regarding accuracy, Table III illustrates a comparison with other published works. Although [1]-[2] and [4] have been designed for higher flow rates, which are less restrictive, it is possible to appreciate a performance for the proposed work in the same order, comparing at minimum and maximum flow rates and at room temperature (same conditions than these published works). Thus, [1] achieves an uncertainly of 1.17% at 10000 l/h whereas the proposed work achieves 1.10% at 7200 l/h. Similarly, [2] presents an uncertainly of 1.99% at 5000 l/h and the proposed work 1.22% at the same flow rate. Moreover, unlike these works, the proposed sensor includes additional features, such as temperature compensation and the implementation of a low cost and low power solution comparing with these other designs, as described in Section I.

TABLE III
UNCERTAINLY COMPARISON RESULTS

	Uncertainly at minimum flow rate	Uncertainly at maximum flow rate
Proposed work	4.41% @40l/h	1.10% @7200l/h
[1]	1.17% @10m^3/h	0.55% @800m^3/h
[4]	-	2.5% @150-500m^3/h
[2]	1.99% @5-50m^3/h	0.51% @50-500m^3/h

Finally, a comparison with an ultrasonic flow sensor in a similar flow range [3] is drawn in Table IV, with the results provided from the average of 6 measurements required by the standard and for the flow rates given by [3]. Although both sensors achieve accuracy results in the same order, note that [3] does not provide results regarding power consumption or accuracy with temperature variations. Moreover, regarding zero flow drift, [3] achieves an error of ±5 ns, higher than the ±0.7 ns achieved in this work and reported in Section III.B.

TABLE IV
ACCURACY COMPARISON RESULTS

	40l/h	1440l/h - 1600l/h	4000l/h
Proposed work	1.80%	0.25%	0.40%
[3]	1.67%	1.09%	0.74%

V. CONCLUSION

A fully designed transit-time based gas flow sensor, with temperature compensation capabilities, enhanced ultrasonic signal sensitivity and minimized power consumption, has been presented in this paper. Accuracy and power consumption have been optimized by the analysis and integration of each design part, by properly selecting the mechanical dimensions, the piezoelectric transducers and the cross-correlation based method by implementing the Hilbert Transform, in order to improve its performance regarding ToF estimation. Exploiting this achieved accuracy, absolute ToFs are employed to implement a novel and low cost temperature compensation method. The proposed design presents accuracy and power consumption features placed into the state-of-the art, meaning a suitable low cost and low maintenance alternative to be integrated to smart IoT gas meters.

REFERENCES

[1] Y. Jiang *et al*., "A Model-Based Hybrid Ultrasonic Gas Flowmeter," *IEEE Sensors J.*, vol. 18, no. 11, pp. 4443-4452, Jun. 2018.
[2] Y. Jiang *et al*., "A Model-Based Transit-Time Ultrasonic Gas Flowrate Measurement Method," *IEEE Trans. Instrum. Meas.*, vol. 66, no. 5, pp. 879-887, May 2017.
[3] J. Chen *et al*., "Design of a High Precision Ultrasonic Gas Flowmeter," Sensors, vol. 20, pp. 1-15, Jun. 2020.
[4] Q. Chen, W. Li and J. Wu, "Realization of a Multipath Ultrasonic Gas Flowmeter based on Transit-Time Technique," *Ultrasonics*, vol. 54, no. 1, pp. 285-290, Jan. 2014.
[5] R. C. Baker, *Flow Measurement Handbook: Industrial Designs, Operating Principles, Performance, and Applications*. New York, USA: Cambridge Univ. Press, 2016.
[6] J. Drachmann, "Ultrasonic flow meter with temperature compensation," European Patent EP 2 000 784 A1, Dec. 10, 2008.
[7] W. Gao *et al*., "Temperature Compensation and Amplitude Prediction in Ultrasonic Measurement Based on BP Neural Network Model," *International Conference on Intelligent Computing and Human-Computer Interaction (ICHCI)*, Sanya, China, Dec. 2020.
[8] X. Tang, Q. Yang and Y. Sun, "Gas flow-rate measurement using a transit-time multi-path ultrasonic flow meter based on PSO-SVM," *IEEE International Instrumentation and Measurement Technology Conference (I2MTC)*, Turin, Italy, May 2021.
[9] J. R. G. Oya *et al*., "Low-power transit time-based gas flow sensor with accuracy optimization," Sensors, vol. 22, no. 24, pp. 1-23, Dec. 2022.
[10] D. T. Blackstock, *Fundamentals of Physical Acoustics*. New York: Wiley-Interscience, 2000, pp. 32–35.
[11] R. Queirós *et al*., "Cross-Correlation and Sine-Fitting Techniques for High-Resolution Ultrasonic Ranging," *IEEE Trans. Instrum. Meas.*, vol. 59, no. 12, pp. 3227-3236, Dec. 2010.
[12] K. Nakahira *et al*., "Distance Measurement by an Ultrasonic System based on a Digital Polarity Correlator," *IEEE Trans. Instrum. Meas*., vol. 50, no. 6, pp. 1748–1752, Dec. 2001.
[13] R. Hanus, "Application of the Hilbert Transform to Measurements of Liquid–Gas Flow Using Gamma Ray Densitometry," *International Journal of Multiphase Flow*, vol. 72, pp. 210-217, Feb. 2015.
[14] Z. Fang *et al*., "Similarity Judgment-Based Double-Threshold Method for Time-of-Flight Determination in an Ultrasonic Gas Flowmeter," *IEEE Trans. Instrum. Meas*., vol. 67, no. 1, pp. 24-32, Jan. 2018.
[15] F. Suñol, D. A. Ochoa and J. E. Garcia, "High-Precision Time-of-Flight Determination Algorithm for Ultrasonic Flow Measurement," *IEEE Trans. Instrum. Meas*., vol. 68, no. 8, pp. 2724-2732, Aug. 2019.